AN APPROACH TO TILTROTOR WING AEROSERVOELASTIC OPTIMIZATION THROUGH INCREASED PRODUCTIVITY

Martin Stettner* and Daniel P. Schrage**
School of Aerospace Engineering
Georgia Institute of Technology
Atlanta, Georgia 30332-0150

Abstract

The paper describes one way to approach the multidisciplinary task of optimizing a tiltrotor wing structure which is equipped with an active flutter suppression system. Objective function is a productivity index, as a measure for aircraft cost-effectiveness. Short digress is held on the characteristics of the tiltrotor's dynamic system and its aeroelastic behavior. Contributing analyses (CA's) for calculating aircraft performance, modeling the dynamic system, and designing an active flutter suppression control system are selected. Multilevel and non-hierarchic decomposition techniques are discussed. A file structure for handling data transfer between the CA's and the optimizer is presented. Preliminary results are shown which highlight some peculiarities of this optimization problem.

Nomenclature

$\overline{A}$	state space system dynamics matrix
ACP	aircraft plant model block
[AIC]	matrix of unsteady aerodynamic influence coefficients
$[A_i]$	coefficient matrix i in Padé - approximation
$\overline{B}$	state space system controls matrix
c	wing chord
[C]	damping matrix
$\overline{C}$	state space system output matrix
CSSO	concurrent subspace optimization
CA	contributing analysis
CSD	analysis module: control system design
DLM	analysis module: unsteady aerodynamics using Doublet-Lattice-Method
ELAPS	analysis module: equivalent plate model of the wing structure
GSE	global sensitivity equation
J	cost function
k	reduced frequency
K	vector of values unchanged in the optimization
KS	Kreisselmeier-Steinhauser function
[K]	stiffness matrix
LQG	Linear Quadratic Gaussian theory
LQR	Linear Quadratic Regulator theory
[M]	mass matrix
PADE	analysis module: Padé-approximation of unsteady aerodynamics
PASTA	analysis module: coupling of aircraft, wing, rotor, and unsteady aerodynamics
PER	performance block
PI	productivity index
q	dynamic pressure
Q	weighting matrix
R	weighting matrix
s	Laplace-variable
[S]	local sensitivity matrix
SSO	subspace optimization
TR	tiltrotor aircraft
u	system controls vector, state space
U	velocity
v_{bl}	block speed
v_c	cruise speed
v_D	dive speed
VDTR	variable diameter tiltrotor
VASCOMP	analysis module: mission analysis, calculation of fuel weight required
W_f	fuel weight
W_{oe}	operational empty weight
W_p	payload weight
W_w	wing weight
WWT	analysis module: wing weight calculation
x	system state vector, state space
x_{AF}	vector of airframe states (wing elastic and rigid body modes)
x_G	vector of gust states (Dryden spectrum)
x_R	vector of rotor states
x_{RC}	vector of rotor control states
x_{WC}	vector of fixed wing control states
X	vector of design variables
y	system output vector, state space
Y	vector of behavior variables

1. Introduction

In the past decade, increasing airport congestion led to reconsideration of vertical take-off and landing (VTOL) configurations for civilian applications. Both in the United States and Europe the tiltrotor (TR) aircraft has received special attention in this context. Considering performance and handling qualities, the aircraft promises to perform similar to a helicopter in hover and low speed forward flight, and close to a turboprop aircraft in cruise.

* Graduate Student
** Professor, Aerospace Engineering
Member AIAA

Additionally, the demonstrator aircraft, XV-15, has proven to be very successful in extensive flight testing, and the larger and more advanced V-22 may be approaching series production. Conversion from helicopter to aircraft mode can be performed in a comparably large range of speeds (wide conversion corridor) and does not cause stability problems. Thus, tiltrotor technology can be considered well proven and safe.

One important aspect in the design of tiltrotor (TR) wings is aeroelastic considerations. In high speed forward flight destabilizing aerodynamic forces on the rotor can lead to a low frequency instability called whirl flutter. The rotor performs a whirling motion which excites both elastic airframe and rigid body modes[1]. To date, research in this area has been concerned with increasing whirl flutter speed by rotor and wing design[2,3] (in general by stiffening of the wing, causing a weight penalty), or by implementation of an active control flutter suppression system for a given configuration[4-7]. In the light of future commercial applications, extensions of this work in two directions are desirable.

First, productivity and cost effectiveness are much more important than sheer speed in the civilian market. Hence, the aircraft should be optimized for maximizing the productivity index, PI,

$$PI = \frac{\text{Payload } W_p \times \text{Block Speed } v_{bl}}{\text{Empty Weight } W_{oe} + \text{Fuel Weight } W_f}$$

(as an indicator for cost effectiveness), thus including favorable effects of increased cruise speed, and drawbacks by the associated rise in structural weight and fuel required.

Second, investigations of fixed-wing flutter suppression systems have indicated that integrated optimization of wing structural configuration and flutter suppression control law yields higher flutter speeds than those obtained from independent optimizations, e.g. a control law optimization for an 'optimized' wing structure[8]. Therefore, wing structure and control system should be optimized simultaneously in order to prevent suboptimal results.

The present approach attempts to cover these two aspects by using multidisciplinary design optimization (MDO) techniques. The overall objective can be described as follows:

"Vary a set of design variables describing the structure of a composite tiltrotor wing such that for a specified mission the productivity index PI is maximized. Design a flutter suppression controller using rotor controls, flaperon and elevator deflection to keep the aircraft free from proprotor whirl and fixed-wing flutter cases and to minimize rms gust response. Ensure that the configuration is feasible with respect to constraints imposed by the mission to be flown (power available), structural integrity in limiting static load cases, and control system activity / actuator saturation. Investigate the impact of replacing a baseline proprotor by a variable diameter design (VDTR). Perform this task with as little computational effort as possible."

Three major analysis components can be identified as necessary for this task: (1) A performance analysis supplying data needed for calculation of the productivity-related objective function; (2) a "plant model" of the aircraft containing structural analysis of the wing, coupling of the wing with fuselage and rotor dynamics, as well as wing unsteady aerodynamics; and (3) a control algorithm calculating the feedback gains required to meet the objectives. Obviously, this optimization problem does not represent a full scale optimization for maximum productivity; in order to simplify the problem, only a restricted set of design variables will be used. More specifically, it will be attempted to determine a wing structure and cruise speed maximizing the productivity index of a EUROFAR-type 30 PAX TR configuration on a representative 2 x 300nm radius mission[9], see Fig. 1 (EUROFAR = EUROpean Future Advanced Rotorcraft). A more detailed description of the optimization problem and the analysis modules required is presented in the following section.

2. Contributing Analyses (CA's)

Considerable time was spent on definition of the exact tasks and selection of analyses, algorithms, and off-the-shelve computer codes for each of the three blocks mentioned above. The following paragraphs highlight a few of the considerations involved in the decision process.

Performance

Two tasks can be defined as part of the performance analysis: (1) calculation of the actual weight of the wing as a function of design variables describing the outer shape of the wing (in the following called "planform") and its internal layout, in order to get the actual empty weight of the aircraft; (2) mission analysis to yield fuel weight required and block speed (payload fixed).

Wing Weight Calculation, WWT

Determination of the wing weight by the module WWT is a straightforward process: first the weight of the load-carrying wing parts as described by design variables is calculated, then weights for flaps, actuators, etc. are added using regression formulas. This total wing weight W_W is then used to find the actual empty weight of the aircraft, which is an input to the mission analysis.

Mission Analysis, VASCOMP

Here, the fuel weight required to perform a representative EUROFAR-mission[9] (Figure 2) is calculated,

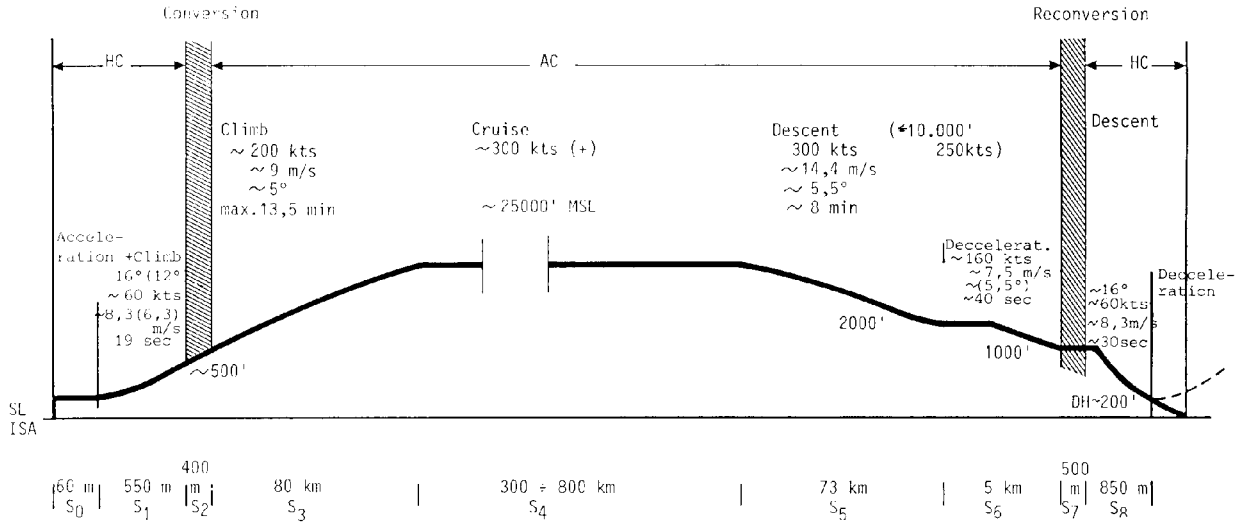

Fig. 1: Representative EUROFAR Mission (taken from von Reth et al.[9])

and it is checked if the aircraft power available (EUROFAR-baseline[10]) is sufficient to hover out of ground effect (HOGE) at 500m ISA +10°, with full mission fuel and payload (equivalent to design gross weight). A ready-to-use tool for this problem is VASCOMP[11], the latest release even includes a model for a variable-diameter tiltrotor (VDTR). However, data input is cumbersome, and the program's flexibility might increase computational effort unnecessarily. For these reasons, a "hard-wired" mission analysis, tailored to this specific application, is in preparation. The decision wether or not to use this code will be made after comparisons of accuracy and CPU time with VASCOMP.

Aircraft Plant Model

This module will supply information about the dynamic properties of the aircraft and its structural integrity in selected static load cases. No single computational tool for this objective is available, so that it is broken down in four subtasks:

Wing Modeling, ELAPS

In contrast to other approaches to aeroelastic modeling, a finite-element code was not considered to be appropriate for this research, due to the large amounts of computer time required, and size of the programs. Instead, an equivalent plate model of the wing was chosen, since it represents a reasonable compromise of accuracy and computational effort[12]. The associated program ELAPS[13], which has proven its applicability to tailoring of composite wings, performs a modal analysis of the wing's dynamics. A supplement to this code checks structural integrity in a 2.0g jump-take-off condition, which in comparative studies showed to be the severest static load condition.

Unsteady Aerodynamics, DLM

Previous research on tiltrotor aeroelasticity utilized quasi-steady theory to model the aerodynamic forces on the oscillating wing[2, 4-7]. However, analysis of van Aken's results[6] indicates that the reduced frequencies occurring in the flutter case (up to k=0.17) do not allow such a simplification. This fact is even more important if swept, anisotropic wings are considered, since in this case pure fixed wing flutter might be encountered (usually, a coupled rotor-wing instability dominated by proprotor whirl flutter would be expected to occur first). Hence, a truly unsteady aerodynamics model is required. A doublet-lattice code is preferred vs. a lifting line method since modeling of the influence of oscillating control surfaces is more straightforward. The program will calculate the aerodynamic influence coefficient matrices with the wing modes as system states (modal AIC = modal aerodynamic influence coefficient matrix) for dive speed 1.15 v_D.

Padé Approximation of Unsteady Aerodynamics, PADE

The modal AIC is in fact a function of reduced frequency, or for non-harmonic motion, of the Laplace-variable s; in order to allow an eigenvalue analysis of coupled aeroelastic systems, and to enable utilization of state-space control system design methods, the functional dependency of these matrices from s is approximated by a Padé-expansion

$$[AIC(s)]=[A_0]+[A_1]\frac{cs}{2U}+[A_2]\left(\frac{cs}{2U}\right)^2+\sum_{m=1}^{L}\frac{[A_{m+2}]\,s}{s+(2U/c)\,b_m}$$

By using the values of [AIC(s)] at the lowest wing natural frequencies and least-squares curve-fitting the coefficient matrices $[A_i]$ of this expansion can be determined. This procedure is performed for AIC

contributions from both wing modes and control.surface deflections.

Rotor Dynamic Model and Coupling of Dynamic Subsystems, PASTA

The procedure described so far is equivalent to that for pure fixed wing aeroservoelastic analysis. Peculiar to the TR is the coupling with the complex dynamic system of a propeller / rotor (proprotor) at the wing tips. Several programs modeling this coupled system are available[1, 2, 14-16]. In the rotorcraft community, CAMRAD[15,16] (and the improved version CAMRAD/JA) is widely accepted as a reference for rotor modeling, offers a TR model as an option, and has already been used for TR aeroelastic analysis[6, 7]. However, CAMRAD is also known for somewhat complicated data input, and its comprehensiveness was considered a drawback within an optimization framework. Instead, the Proprotor Aeroelastic STability Analysis PASTA[1] was chosen as a baseline for a program tailored to the specific requirements of this optimization task. PASTA already utilizes input of modal wing data, but addition of rotor controls, inclusion of wing unsteady aerodynamics, and incorporation a rigid body model capable of modeling short period longitudinal dynamics* require modifications. These modifications should not present a problem though, since the FORTRAN source code is available and the theory behind the code is described in detail in Kvaternik's PhD Dissertation[1]. Furthermore, the source code can be extended to accommodate conversion of the coupled rotor-airframe-aerodynamics system**

$$\left([M]s^2+[C(q)]s+[K(q)]\right)\begin{Bmatrix} x_{AF} \\ x_R \\ x_{RC} \end{Bmatrix} + q[AIC(s)]\begin{Bmatrix} x_{AF} \\ x_{WC} \\ x_G/U \end{Bmatrix} = 0$$

into the state-space representation standard form

$$\dot{x} = \bar{A}\,x + \bar{B}\,u$$
$$y = \bar{C}\,x$$

which is handed down to the controls system design CA.

Control System Design, CSD

Goal of this CA is to design a constant gain feedback controller which allows an optimum of stability, minimal rms gust response, and robustness with respect to the aircraft's flight condition. Three different approaches to designing such a flutter suppression controller were identified in a literature research: Eigenspace techniques[17], the Aerodynamic Energy Concept[18], and Linear Quadratic Gaussian Theory[e.g.19]. Eigenspace techniques require specification of desired system pole locations in the complex plane; but pole placement in the light of robustness and minimal gust response requires a very good knowledge of the plant, and the plant characteristics might change significantly during the optimization. Controllers designed using the Aerodynamic Energy Concept and LQG theory have been compared in wind tunnel tests and showed comparable performance and robustness with respect to velocity[20]. If control effort is considered, LQG theory provides readily the information required since a quadratic measure of control system activity u, weighted by the matrix R, is already part of the cost function

$$J = \int_0^\infty \left(x^T Q\, x + u^T R\, u\right)\, dt$$

and is therefore preferable. However, in reduced - state LQG design more than half of the effort is to find a robust Kalman Filter which reconstructs all system states while approximating the stability margins provided by a full-state Linear Quadratic Regulator (LQR). In the optimization framework it appears to be more appropriate to assume that this filter design can be accomplished, and to reduce the problem to LQR design. In this case, stability would be guaranteed (under the premise of detectability and stabilizability), and gust response and control system activity could be minimized by varying the ratios of elements in the Q matrix to those in the R matrix. This method requires a priori knowledge of some plant characteristics ("roundness" of the plant) in order to choose the appropriate size of elements within the R and Q matrix. A second approach is to simply chose certain feedback channels and to optimize the gains in these channels.

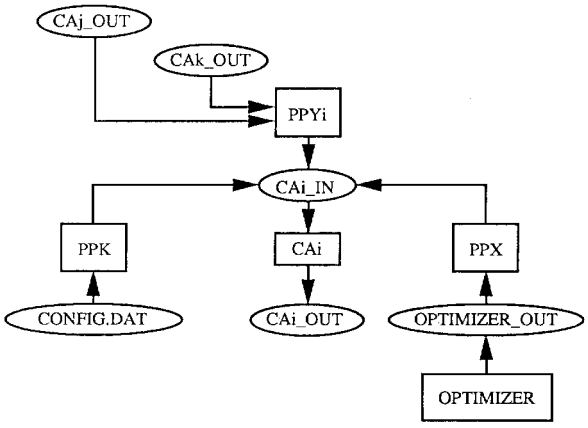

Fig. 2: Data Transfer Schematic

* Whirl flutter includes low frequency modes, which may couple into flight mechanic degrees of freedom, especially the short period oscillation.

** The damping matrix [C] and the stiffness matrix [K] are only a function of dynamic pressure q for rotor states and controls, indicating quasi-steady aerodynamics.

CA	Input X (VDTR in italics)	Y	K	Output Y	to PI calculation (constraints)
WWT	wing planform; wing int. layout	-	material density; W_{oe} w/o wing	empty wt. W_{oe}	empty wt. W_{oe}
VASCOMP	wing planform; cruise speed v_C; *(rotor hover/cruise diameter)*	empty wt. W_{oe}	mission profile; ac. configuration	fuel wt. W_f; dive speed v_D	fuel wt. W_f; block speed v_{bl} (power required vs. power av.)
ELAPS	wing planform; wing int. layout	fuel wt. W_f	wing material density and elastic properties; nacelle inertial properties	wing eigenvalues, eigenvectors, gen. masses (lowest)	(structural margin of safety, static load cases)
DLM	wing planform	wing eigenvalues, eigenvectors, gen. masses; dive speed v_D	air density	modal aerodynamic influence coefficient matrices (AIC) at wing natural frequencies	-
PADE	-	modal AIC matrices;	-	Padé approxim. AIC matrices	-
PASTA	*(rotor cruise diameter)*	wing eigenvalues, eigenvectors, gen. masses (lowest); Padé approxim. AIC matrices	rotor configuration sensor location	state-space system dynamics, output, and control matrix	-
CSD	-	state-space system dynamics, output, and control matrix	-	-	(rms gust response, states and controls)

Table 1: CA Data Input and Output

Insight to the most effective feedback channels is provided by the work of Frick and Johnson[4]. Both approaches are being considered, the second one mainly because of its simplicity.

3. CA Data Transfer Structure and Sensitivity Analysis

Table 1 provides an overview of the data transfer between the different CA's. The terminology is chosen to be similar to that used by Sobieszczanski-Sobieski[21]: Each CA receives input data from the optimizer (design variables X), other CA's (behavior variables Y), and from a configuration data base (constants K). Fig. 2 sketches how data will be transferred between the CA's and the optimizer (CONMIN[22]) without utilization of a data base code:

At the beginning of an optimization, a preprocessor (PPK) reads data, which are not to be changed during the optimization (vector K), from a database file (CONFIG.DAT), and writes them in the proper format in CA input files (CAi_IN). After each step of the optimizer, the new design variables X, contained in the optimizer output file (OPT_OUT), are distributed in the CA input files by another preprocessor (PPX). Finally, before a certain CAi is started, a preprocessor specific to that CA (PPYi) transfers the remaining data (behavior variables Y) from output files of other CA's (CAj_OUT, CAk_OUT) into the input file. This process is controlled by an operating system batch file. Goal of the procedure is to reduce the number of read-write processes.

In Fig. 3, the connections between the CA's (i.e. the exchange of behavior variables, as described in the preceding section and summarized in Table 1) are displayed in an Nsquare diagram, which allows analysis of hierarchies amongst the CA's. Top-down data transfer (feed forward) is indicated by connections above and right of the main diagonal, and it becomes apparent that no iteration will be necessary, since there are no feedback links under the main diagonal. This feature can be mainly attributed to simplifications in the analysis, e.g. the neglect of actuator weight change as a function of control system activity, which would feed back into the aircraft plant model. In this approach however the actuators are assumed to be given (configuration fixed), so that actuator weight is not a behavior variable. This assumption also appears to be a very practical one, since the question could be asked as to how good stabilization and gust alleviation can be performed with a certain set of baseline actuators.

The most important feature of the Nsquare Diagram however is to indicate a hierarchy amongst the CA's. Fig. 3 represents already a "processed" version of an Nsquare diagram, since the CA's have been placed on the diagonal according to their position in the hierarchy, with the highest

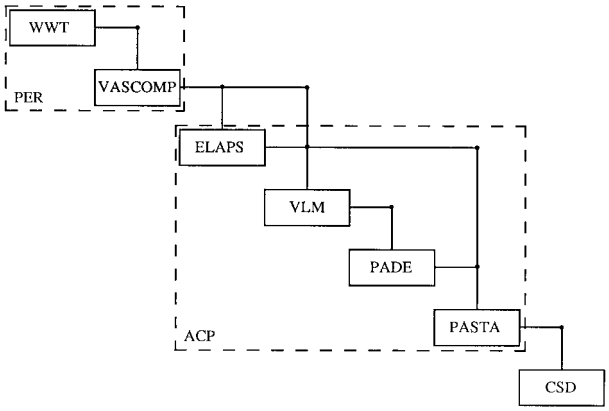

Fig. 3: Nsquare Diagram

level in the upper left corner, and the lowest one in the lower right. With this tool at hand, the question how to approach the sensitivity analysis of this system can be discussed. Five different options of increasing structural complexity are discussed as follows.

(1) The simplest approach is obviously to consider all seven CA's as one analysis, and to wrap a finite-differencing scheme around them to obtain sensitivities of objective function (PI) and constraints with respect to the design variables. This procedure is very inefficient in the best case, and leads to suboptimal results in the worst case[23].

(2) The next step in structural complication of the sensitivity calculation is represented by non-hierarchic decomposition: local sensitivities of CA outputs with respect to CA inputs are obtained either by finite differencing or (semi-) analytic methods (theory available, e.g. for aerodynamics[24] and LQG controller design[25]); the global sensitivities (total derivatives of CA outputs with respect to design variables) are then calculated by solution of the Global Sensitivity Equation GSE[21] for determining objective function and constraint sensitivities. Fig. 4 shows this GSE formulation on the basis of sensitivities of individual CA's (GSE2 according to Sobieszczanski-Sobieski[21]) for the specific application described. A change in the problem structure by adding feed-forward or feedback links between the CA's could be handled without major changes in the GSE, since only the zero-elements in question in the matrix of local sensitivities needed to be replaced by the appropriate derivatives. However, the flexibility of this approach is directly linked with the fact that all local sensitivities enter the GSE. Considering that each element in the matrix of Fig. 4 is a matrix itself, computational cost involved for solution of this GSE becomes a concern.

(3) An improvement is possible by using the hierarchic order displayed in the Nsquare diagram, Fig. 3, andperforming multilevel optimization. In this case,

$$[S]\left(dY / dX_k\right) = \left(\partial Y / \partial X_k\right)$$

$$[S] = \begin{bmatrix} I & & & & & & \\ -\frac{\partial Y_{VASCOMP}}{\partial Y_{WWT}} & I & & & & & \\ & -\frac{\partial Y_{ELAPS}}{\partial Y_{VASCOMP}} & I & & & & \\ & -\frac{\partial Y_{VLM}}{\partial Y_{VASCOMP}} & -\frac{\partial Y_{VLM}}{\partial Y_{ELAPS}} & I & & & \\ & & & -\frac{\partial Y_{VLM}}{\partial Y_{PADE}} & I & & \\ & & \frac{\partial Y_{PASTA}}{\partial Y_{ELAPS}} & & -\frac{\partial Y_{PASTA}}{\partial Y_{PADE}} & I & \\ & & & & & & I \end{bmatrix}$$

$$\left\langle \frac{dY}{dX_k} \right\rangle = \begin{pmatrix} \frac{dY_{WWT}}{dX_k} \\ \frac{dY_{VASCOMP}}{dX_k} \\ \frac{dY_{ELAPS}}{dX_k} \\ \frac{dY_{VLM}}{dX_k} \\ \frac{dY_{PADE}}{dX_k} \\ \frac{dY_{PASTA}}{dX_k} \\ \frac{dY_{CSD}}{dX_k} \end{pmatrix}; \quad \left\langle \frac{\partial Y}{\partial X_k} \right\rangle = \begin{pmatrix} \frac{\partial Y_{WWT}}{\partial X_k} \\ \frac{\partial Y_{VASCOMP}}{\partial X_k} \\ \frac{\partial Y_{ELAPS}}{\partial X_k} \\ \frac{\partial Y_{VLM}}{\partial X_k} \\ \frac{\partial Y_{PADE}}{\partial X_k} \\ \frac{\partial Y_{PASTA}}{\partial X_k} \\ \frac{\partial Y_{CSD}}{\partial X_k} \end{pmatrix}$$

Fig. 4: Global Sensitivity Equation (GSE2)

different objective functions are assigned to blocks of CA's (or only single CA's) - of course, at the uppermost level, this being the overall objective function. According to the sensitivity of the block objective function to the design variables, subsets of design variables are assigned to different blocks. Then, this subset of design variables is perturbed in order to optimize the block objective function, where behavior variables handed down from blocks in higher levels are considered as constants[26]. Fig. 3 displays clearly that the present system could be decomposed in seven levels, but this attempt would be ill - fated for several reasons: (a) designation of design variables becomes somewhat subjective - only assignment of feedback gains to CSD and cruise speed to VASCOMP is straightforward; the remaining few variables, which describe the wing, must be distributed on the other five CA's); (b) the computational cost involved in seven optimizer runs per optimization step might not be worth the effort; (c) even if it would pay off in computational effort per optimizer step, it can be expected that the overall convergence rate will suffer, since the sublevel optimizations will force the search at least initially in a wrong direction; and most important: (d) What should the seven objective functions be?

(4) A good compromise between the extremes described in the two paragraphs above is to combine WWT and VASCOMP in a performance block PER, ELAPS, DLM, PADE, and PASTA in an aircraft plant model block ACP, and leave CSD as a single block (see Fig. 3). In PER, wing design variables describing the outer shape (like sweep and relative thickness) are perturbed to obtain a maximum in PI.

Within ACP, safety margins in 2.0g jump-take-off, 10g landing, and 3.5g pull-up conditions are maximized (by varying ply thickness, ply orientation, and spar cap thickness). Finally, CSD provides a stabilizing feedback controller which minimizes rms gust response, where feedback gains (or the Q and R weighting matrices in the case of the LQR design) are design variables. Within PER and ACP, the GSE2 is used to determine sensitivities. Concerns about the effect of the choice of objective functions in each analysis block on convergence rate remain for this variant.

(5) These problems can be effectively encountered by applying methods related to Concurrent Subspace Optimization (CSSO)[27]: Instead of optimizing for a different objective function in each analysis block (or subspace), maximization of PI (or minimization of constraint violation) is the goal in all subspaces. Constraints from all subspaces are considered in each subspace optimization (SSO). A set of coefficients in the constraints define the "responsibility" of one subspace to reduce violation of certain constraints, acceptability of constraint violation in this subspace, when it is possible to compensate in another ("trade-off"), and "switching" between these two options. Aside from the optimization of "physical" design variables in the SSO's, these coefficients are to be determined in a separate optimization problem. Obviously, this approach has advantages concerning convergence per optimization step, but it also adds complexity and computational intensity involved in each step. (Note that in this specific application utilization of the Kreisselmeier-Steinhauser (KS) function to represent multiple constraints within each SSO in a single cumulative constraint measure[28] is only necessary in CSD, where optimization for minimum rms system and controls gust response is replaced by a constraint on these values. Thus, in CSD stability and gust response are combined in a KS function, whereas in ACP only minimum safety margin, and in PER power required qualify as constraints. Furthermore, the SSO in CSD is only concerned with minimization of constraint violation, since the feedback gains - design variables in this SSO - have no direct influence on the value of PI.)

It was decided that both options (3) and (4) represent a reasonable compromise of complexity and convergence speed. Comparison of these two approaches will lead to a final decision.

4. Preliminary Trend Studies

In order to obtain some a priori information about sensitivity trends in TR wing optimization, two simplified system optimizations were performed. Both studies have the following features in common:

- Powell - type, unconstrained optimization algorithm; therefore no calculation of sensitivities within the optimization
- exponential penalization of constraint violation
- no wing aerodynamics
- wing represented by a rectangular composite anisotropic wing box[29], wing mass neglected with respect to nacelle mass in calculation of wing modes
- reduced number of internal wing structure design variables (Fig. 5), wing box thickness fixed
- no in-plane rotor degrees of freedom
- no aircraft rigid body degrees of freedom
- no control system

Loewer[30] analyzed optimization for maximum PI with a rudimentary performance model. It was assumed that in the baseline case the aircraft would fly with minimum drag at 335kts. Additional speed increases the zero lift drag coefficient due to compressibility influences, which can be reduced by variation of wing sweep. Fig. 6 to 11 are results of an optimization run in which PI was increased by about 40% of the baseline value to 86.14 kts. Investigation of these plots leads to the following conclusions:

- *The performance model is too simple:* The "Power Factor" curves in Fig. 6 and 7 (ratio of power required to power available) are neartly identical, despite a wing box weight reduction by more than 53% (or about 750 lbs) to 666 lbs. Deviations in wing sweep from the baseline value of 0° are prevented through increase of wing weight. Increased speed is severly penalized by drag rise, so that the optimized cruise speed deviates hardly from the starting value, but a tendency to a higher cruise speed can be detected (337.14 kts vs. 335 kts). All three observations support the impression that the optimization reduces to wing weight minimization as a result of the simplified drag model. It is expected that optimization with an improved performance model will result in higher cruise speed.

Wing Box Wall Segment Numbers:

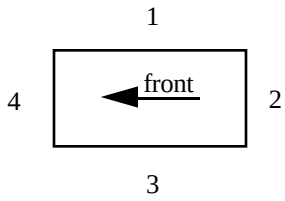

Ply Thicknesses:

	Ply 1: + 45 °	Ply 2: - 45 °	Ply 3: 0 °
1	$\tau_B\, t_T$	$(1-\tau_B)\, t_T$	t_B
2	$\tau_C\, t_T$	$(1-\tau_C)\, t_T$	t_C
3	$(1-\tau_B)\, t_T$	$\tau_B\, t_T$	t_B
4	$(1-\tau_C)\, t_T$	$\tau_C\, t_T$	t_C

Fig. 5: Internal Wing Layout Design Variables

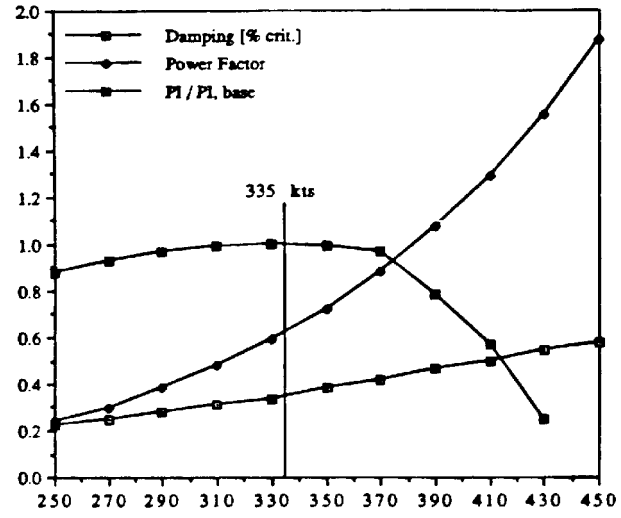

Fig. 6: Sensitivity of Baseline w.r.t. Cruise Speed [kts]

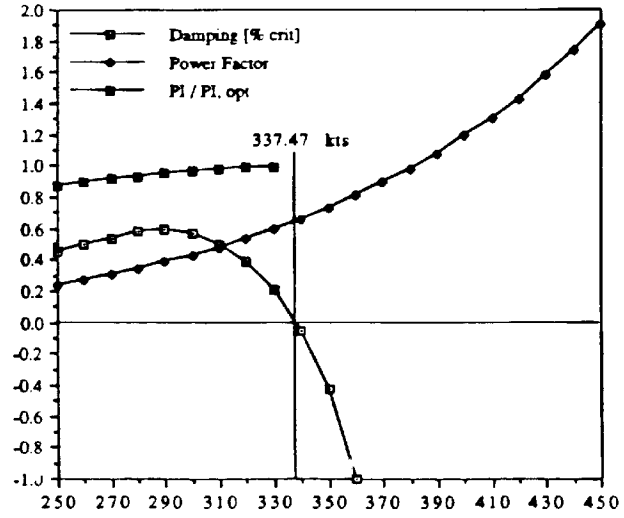

Fig. 7: Optimal Sensitivity w.r.t. Cruise Speed [kts]

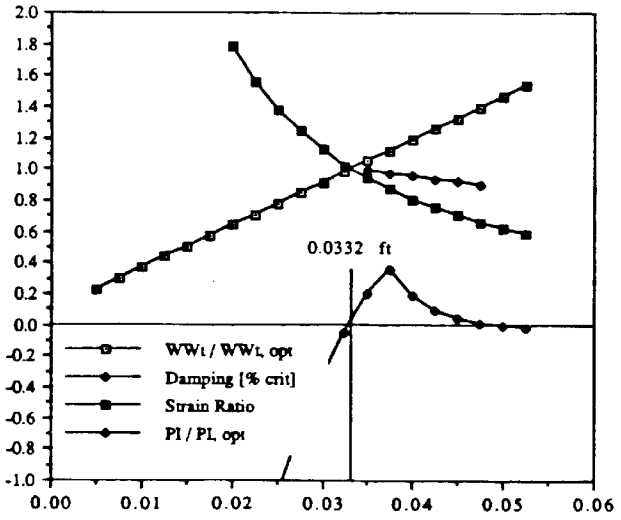

Fig. 8: Optimal Sensitivity w.r.t. t_B [ft]

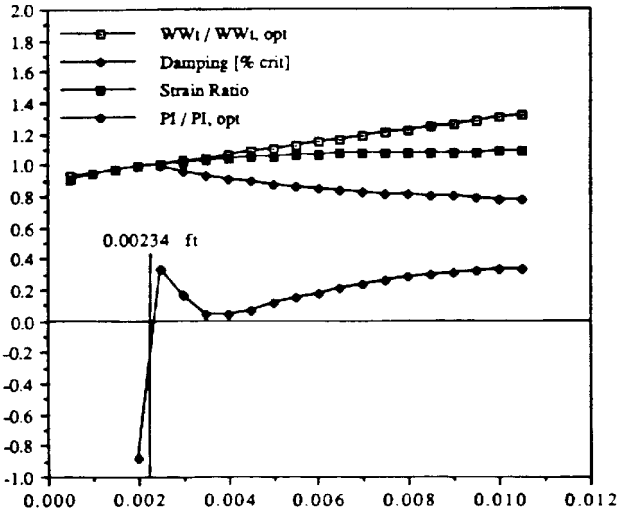

Fig. 9: Optimal Sensitivity w.r.t. t_C [ft]

- *Proprotor whirl is a severe constraint:* Fig. 7 indicates that the optimized configuration cruises close to flutter speed (no safety margins were considered in this case). Feasible values for t_B, t_C, τ_B, and τ_C are limited by the stability constraint (Fig. 8 to 11).

- *Both structural integrity and stability constraints are active in the optimum:* For the optimal value of t_B = 0.0352 ft, Fig. 8 shows strains in the 2.0g jump-take-off condition closing in on admissable values ("Strain Ratio" = 0.99) and damping approaching 0% critical.

- *The least damped mode changes character close to the optimum:* Fig. 8 and 9 display a peak in the damping curve close to the optimal values. Analysis of eigenvectors reveals that left of the peak the critical mode is dominated by wing torsion, with a contribution of the progressing rotor flap mode, whereas to the right of the peak wing beamwise bending is being excited by regressing rotor flapping. Wing chordwise bending is small in both cases.

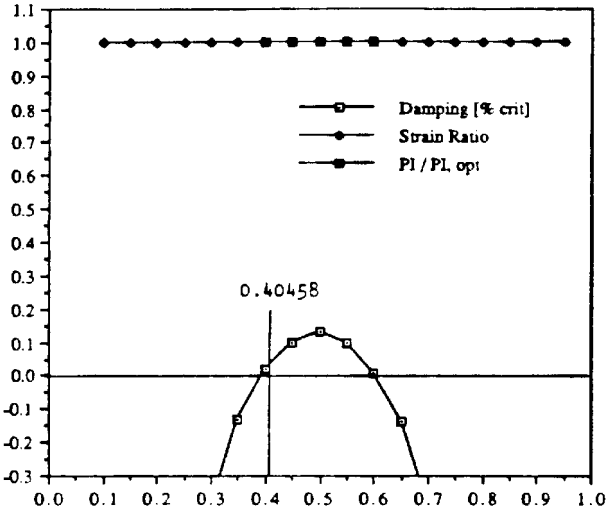

Fig. 10: Optimal Sensitivity w.r.t. τ_C

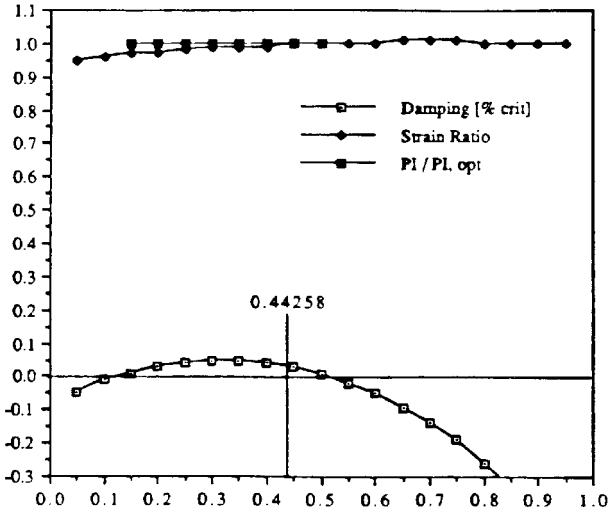

Fig. 11: Optimal Sensitivity w.r.t. τ_B

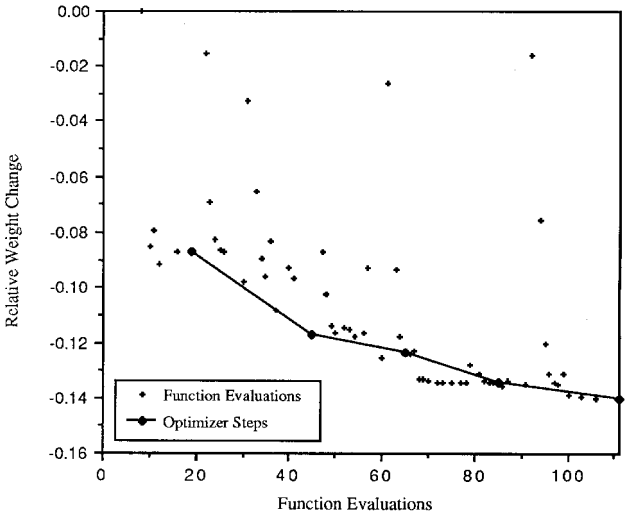

Fig. 12: Wing Weight History

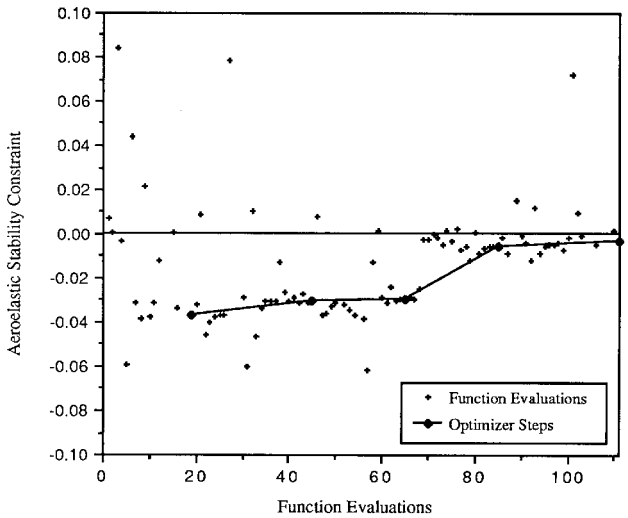

Fig. 13: Stability Constraint History

- *Elastic bending - torsion couplings in the wing are important factors for proprotor stability, and fixed wing aeroelastic stability must be considered:* τ_B and τ_C do not effect PI, but they have significant influence on system damping (Fig. 10 and 11). Remaining stability margins are not exploited, because speed increase is prevented by the dominating drag penalty. Damping alone is maximized by τ_C = 0.5, which means that +45° and -45° layers have equal thickness in the vertical wing box walls. τ_B maximizes damping for values of less than 0.5, which corresponds to plunge up - pitch down coupling in the wing structure. This result is important in that these kinematics decrease fixed wing flutter speed. In other words, a trade-off between rotor whirl and fixed wing flutter cases appears necessary so that inclusion of fixed wing unsteady aerodynamics becomes mandatory.

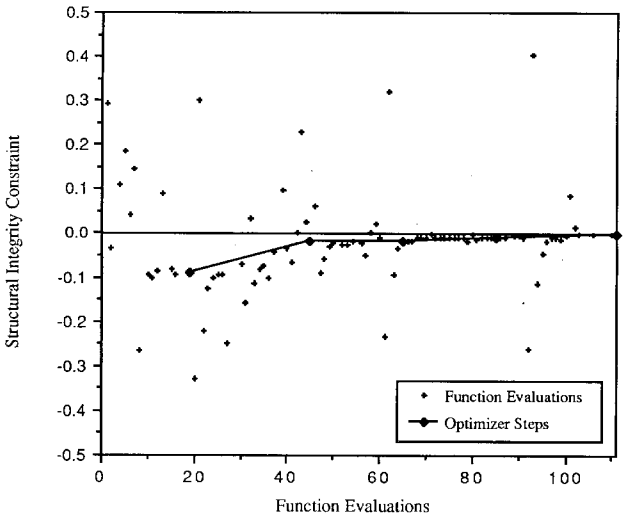

Fig. 14: Structural Constraint History

Due to the deficiencies in the performance model, another study was aimed at pure wing weight minimization (cruise speed held constant), with a stronger focus on static load cases: 2.0g jump-take-off, 10g landing, and 3.5g pull-up were modeled. Objective function and constraint histories are shown in Fig. 12 to 14 (in accordance with common practice, negative values of constraints indicate a feasible configuration; wing weight in Fig. 12 is normalized by the first feasible, i.e. unpenalized value, which occurs at the ninth function evaluation). Again, both the stability and structural integrity constraint are active. This finding is not as straightforward as it might seem, since preliminary design studies seemed to indicate that the 2.0g jump-take-off condition leads to an excessively stiff wing which would prevent whirl flutter. In fact, all data points in Fig. 14 are associated with this condition, the other conditions caused much smaller strains. For future investigations, means to reduce these loads should be analyzed; for example, a strut can reduce root bending moments during take-off, but is also subject to buckling in the landing condition, and increases airframe drag.

5. Concluding Remarks

The preliminary results clearly indicate the necessity for an improved performance model and support the requirement of consistent multidisciplinary modeling. Next step in this research is therefore to replace the present analysis, and to arrange the exsisting codes in the three-block structure of Fig. 3. Stepwise replacement of the other programs with more sophisticated codes and embedded sensitivity investigations will lead to a reliable overall analysis.

6. Acknowledgements

The work presented here is supported by a contract with the Sikorsky Aircraft Division of the United Technologies Corporation.

References

[1] Kvaternik, R.G., "Studies in Tiltrotor VTOL Aircraft Aeroelasticity," PhD Dissertation, Department of Solid Mechanics, Structures, and Mechanical Design, Case Western Reserve, June 1973

[2] Johnson, W., "Analytical Model for Tilting Proprotor Dynamics, Including Blade Torsion and Coupled Bending Modes, and Conversion Mode Operation," NASA - TM - X 62369, August 1974

[3] Nixon, M.W., "Parametric Studies for Tiltrotor Aeroelastic Stability in High-Speed Flight," AIAA/ASME/ASCE/AHS/ASC 33rd Structures, Structural Dynamics, and Materials Conference, Dallas, Texas, April 13-15, 1992

[4] Frick, J., and Johnson, W., "Optimal Control Theory Investigation of Proprotor/Wing Response to Vertical Gust," NASA - TM - X - 62384, September 1974

[5] Nasu, K., "Tilt-Rotor Flutter Control in Cruise Flight," NASA - TM - 88315, December 1986

[6] van Aken, J. M., "Alleviation of Whirl-Flutter on Tilt-Rotor Aircraft using Active Controls," presented at the 47th Annual Forum of the American Helicopter Society, Phoenix, Arizona, May 6-8, 1991

[7] van Aken, J. M., "Alleviation of Whirl-Flutter on a Joined-Wing Tilt-Rotor Aircraft Configuration using Active Controls," presented at the American Helicopter Society International Specialists' Meeting on Rotorcraft Basic Research, Atlanta, Georgia, March 25-27, 1991

[8] Dracopoulos, T.N., "Aeroelastic Control of Composite Lifting Surfaces: Integrated Aeroelastic Control Optimization," PhD Dissertation, The Ohio State University, 1988

[9] von Reth, R.D., Hagmann, U., and Huber, H., "EUROFAR - Projekt für ein senkrecht startendes Reiseflugzeug," Symposium 'Luftfahrt-Städtebau-Umwelt (II)', Aachen, Germany, January 17-18, 1989

[10] Renaud, J., Huber, H., and Venn, G., "The EUROFAR Program: An European Overview on Advanced VTOL Civil Transportation System," 17th European Rotorcraft Forum, Berlin, Germany, September 24-27, 1991

[11] Schoen, A.H., Rosenstein, H., Stanzione, K., and Wisniewski, J.S., "User's Manual for VASCOMP II, The V/STOL Aircraft Sizing and Performance Computer Program," Boeing Vertol Company Report D8-0375, Vol. VI, Third Revision, May 1980

[12] Giles, G.L., "Equivalent Plate Analysis of Aircraft Wing Box Structures with General Planform Geometry," *Journal of the Aircraft*, Vol. 23, No. 11, November 1986

[13] Giles, G.L., "Further Generalizations of an Equivalent Plate Analysis for Aircraft Structural Analysis," *Journal of the Aircraft*, Vol. 26, No. 1, January 1989

[14] Yasue, M., "User's Manual for Computer Program ROTOR - to calculate Tiltrotor Aircraft Dynamic Characteristics," NASA - CR - 137553, August 1974

[15] Johnson, W., "Development of a Comprehensive Analysis for Rotorcraft - I. Rotor Model And Wake Analysis," *Vertica*, Vol. 5, pp. 99-129, 1981

[16] Johnson, W., "Development of a Comprehensive Analysis for Rotorcraft - II. Aircraft Model, Solution Procedure and Applications," *Vertica*, Vol. 5, pp. 185-216, 1981

[17] Liebst, B.S., Garrard, W.L., and Farm, F.A., "Design of a Multivariable Flutter Suppression / Gust Load Alleviation System," *Journal of Guidance*, Vol. 11, May - June 1988, pp. 220-229

[18] Nissim, E., Abel, I., "Development and Application of an Optimization Procedure for Flutter Suppression using the Aerodynamic Energy Concept," NASA - TP - 1137, February 1978

[19] Mukhopadhyay, M., Newsom, J.R., and Abel, I., "Reduced-Order Feedback Control Law Synthesis for Flutter Suppression," *Journal of Guidance*, Vol. 5, No. 4, July-August 1982, pp. 389 - 395

[20] Nissim, E., Abel, I., and Dunn, H.J., "Application of two Design Methods for Active Flutter Suppression and Wind-Tunnel Test Results," NASA - TP - 1653, 1980

[21] Sobieszczanski-Sobieski, J., "Sensitivity of Complex, Internally Coupled Systems," *AIAA Journal*, Vol. 28, No. 1, January 1990, pp. 153-160

[22] Vanderplaats, G.N., "CONMIN - A FORTRAN Program for Constrained Function Minimization," NASA - TM - X - 62282, August 1973

[23] Sobieszczanski-Sobiesky, J., "Multidisciplinary Optimization for Engineering Systems: Achievements and Potential," NASA - TM - 101566, March 1989

[24] Yates, E.C., "Aerodynamic Sensitivities from Subsonic, Sonic, and Supersonic Unsteady, Nonplanar Lifting - Surface Theory," NASA - TM - 100502, September 1978

[25] Gilbert, M.G., "An Analytical Sensitivity Method for Use in Integrated Aeroservoelastic Aircraft Design," NASA - TM - 101583, May 1989

[26] Gilbert, M.G., and Schmidt, D.K., "Integrated Structure / Control Law Design by Multilevel Decomposition," NASA - TM - 101623, June 1989

[27] Bloebaum, C.L., Hajela, P., and Sobieszczanski-Sobiesky, J., "Non-Hierarchic System Decomposition in Structural Optimization," Third Air Force / NASA Symposium on Recent Advances in Multidisciplinary Analysis and Optimization, San Francisco, California, September 24-26, 1990

[28] Sobieszczanski-Sobiesky, J., "Optimization by Decomposition: A Step from Hierarchic to Non-Hierarchic Systems," Second NASA/Air Force Symposium on Recent Advances in Multidisciplinary Analysis and Optimization, Hampton, Virginia, September 28-30, 1988

[29] Badir, A., "Analysis of Advanced Thin-Walled Composite Structures," PhD Thesis, Georgia Institute of Technology, February 1992

[30] Loewer, S., "Sensitivity of Tiltrotor High Speed Performance to Wing Structural Parameters," Diploma Thesis, Technische Universität Braunschweig, April 1992